Electronic Supplementary Material (ESI) for Nanoscale.

Electronic Supporting Information

Phonon-assisted molecular upconversion in a Holmium(III)-based molecular cluster-aggregate

Diogo Alves Gálico,[a] Rayan Ramdani,[a] and Muralee Murugesu *[a]

[a] Department of Chemistry and Biomolecular Sciences, University of Ottawa, Ottawa, Ontario K1N 6N5, Canada.

Email: m.murugesu@uottawa.ca

Experimental Section

Synthesis of {$Gd_8Ho_2Yb_{10}$}: The synthetic procedure follows the previously reported with small adaptations.[S1,S2]

0.4 mmol of $Gd(NO_3)_3 \cdot 6H_2O$, 0.1 mmol of $Ho(NO_3)_3 \cdot 5H_2O$, 0.5 mmol of $Yb(NO_3)_3 \cdot 5H_2O$, and 6-chloro-2-pyridinol (0.130 g, 1.00 mmol) were added in 20 mL of MeOH/MeCN (1:1), followed by the addition of triethylamine (0.139 mL, 1.00 mmol). After 12 hours, the resulting solution was filtered and left undisturbed in an open vial for solvent evaporation under room temperature. Pale yellow block-like single crystals were obtained after 10 days.

ICP analysis: Calculated: Gd (40 %) / Ho (10 %) / Yb (50 %). Obtained: Gd (38.6 %) / Ho (12.1 %) / Yb (49.3 %). Yield = 45 % (crystalline product).

Sample preparation: For the luminescence studies, 10 mL of a 0.1 mg mL^{-1} solution (deuterated methanol) of **{$Gd_8Ho_2Yb_{10}$}** was prepared. For TEM and DLS analysis, 100 µL of this solution was diluted in 900 µL of deuterated methanol.

Characterizations:

FTIR spectra were obtained in a Nicolet 6700 FT-IR Spectrometer (Thermo Scientific).

PXRD diffractograms were obtained in a Rigaku Ultima IV Diffractometer using Cu Kα filtered radiation (λ = 1.5401 Å).

ICP analysis was performed in a 5110 ICP-OES Instrument (Agilent).

DLS spectrum was obtained with a Malvern Zetasizer Nano with a 633 nm laser (DPSS, 50 mW).

Scanning electron microscopy (SEM) and Energy-dispersive X-ray spectroscopy (EDS) were obtained with a JEOL JSM-7500F.

Transmission electron microscopy (TEM) was obtained with a FEI Tecnai G2 F20 TEM applying 120 kV.

Photoluminescence analyses were obtained using a Quanta Master 8075-21 Spectrofluorometer (Horiba) equipped with a red-extended detector (Hamamatsu R13456 red extended PMT) for the visible and a liquid nitrogen cooled InGaS detector for the near-infrared range. The excitation of the samples was performed using a 980 nm CW laser (max power: 2 W) focused with a 62.3 mm focal length lens. The emission

spectra were corrected according to the optical system of the emission monochromator and the photomultiplier response. The quartz cuvette was placed inside a single cuvette Peltier K-155-C kept at 20 °C.

Absolute quantum yields were obtained with a K SPHERE petite integrating sphere and the **{Gd_{20}}** analogue was used as the blank reference (no absorption at 980 nm). The incident laser power was measured with a ThorLabs PM100D compact power meter.

Figures and Tables

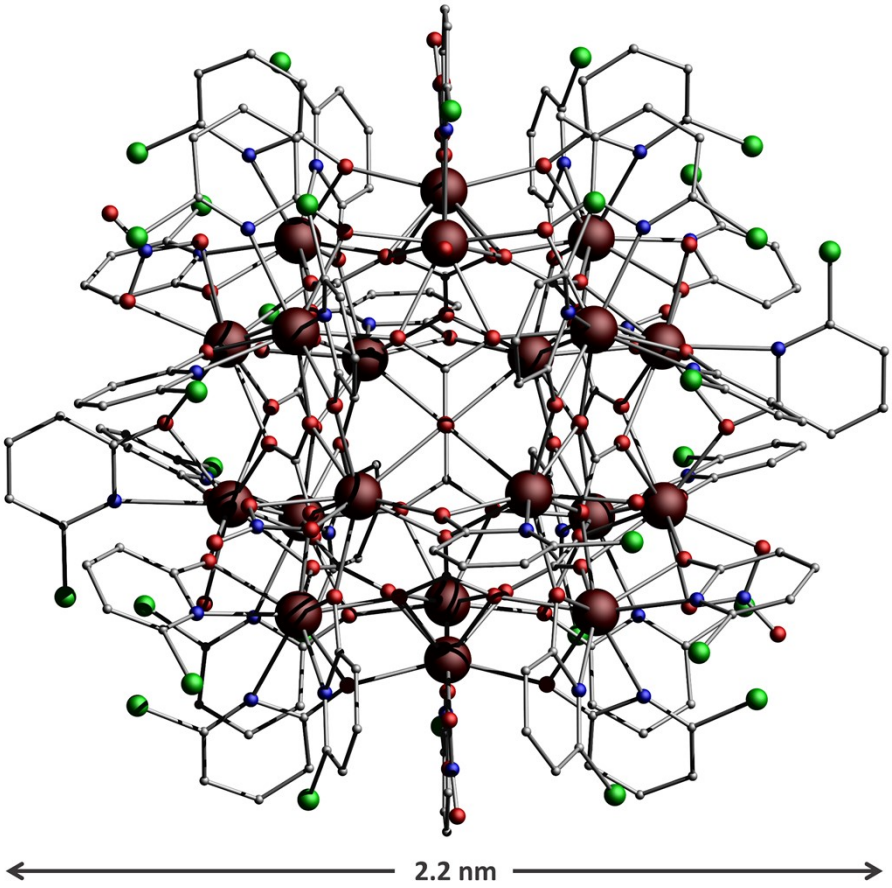

Figure S1: Molecular structure of **{Gd_{20}}** MCA (CCDC number: 1001482). Hydrogen and solvent atoms are omitted for clarity. Colour code: Grey: carbon; Red: oxygen; Blue: Nitrogen; Green: Chlorine; Wine: Gd^{III}.

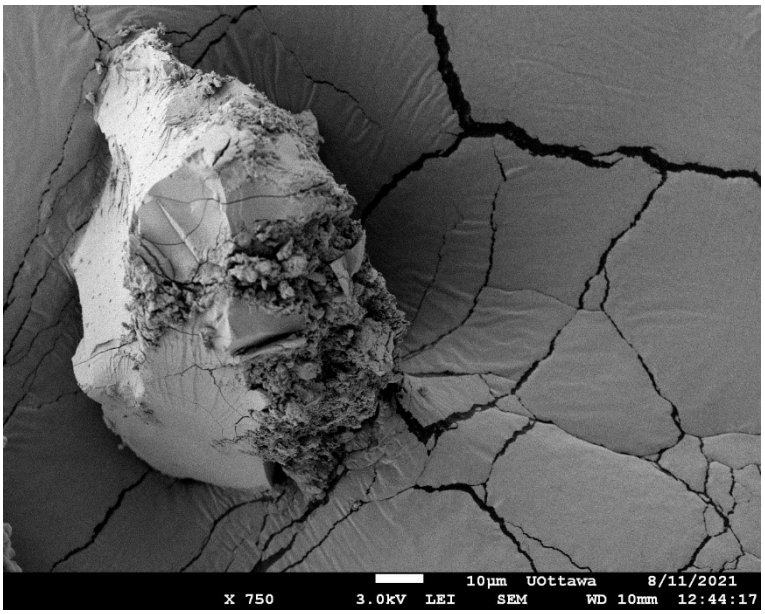

Figure S2: SEM images for **{$Gd_8Ho_2Yb_{10}$}** MCA.

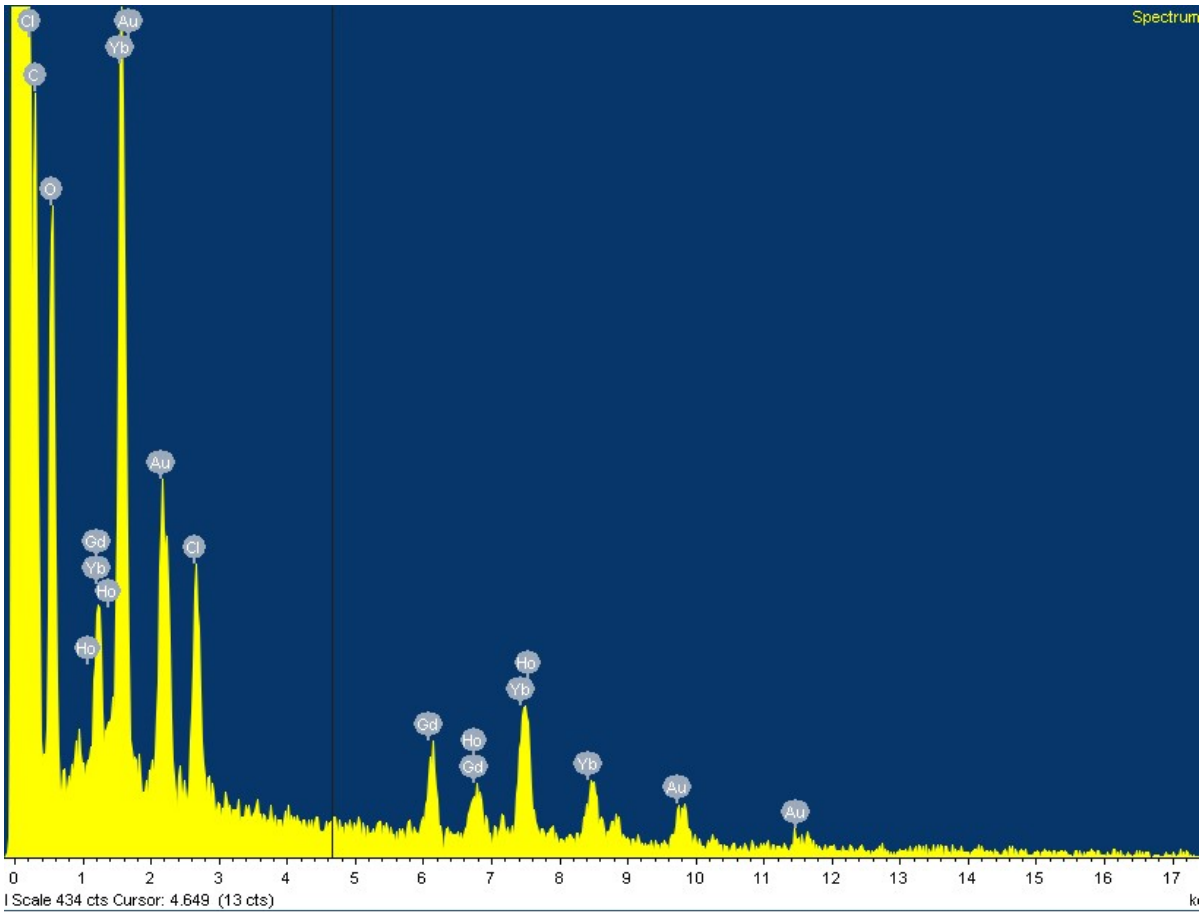

Figure S3: EDS spectra for **{$Gd_8Ho_2Yb_{10}$}** MCA. EDS spectra were used to qualitatively prove the presence of Gd^{III}, Ho^{III}, and Yb^{III} ions. The close proximity of Ho^{III} and Yb^{III} peaks result in signal overlapping, making a quantitative analysis unfeasible.

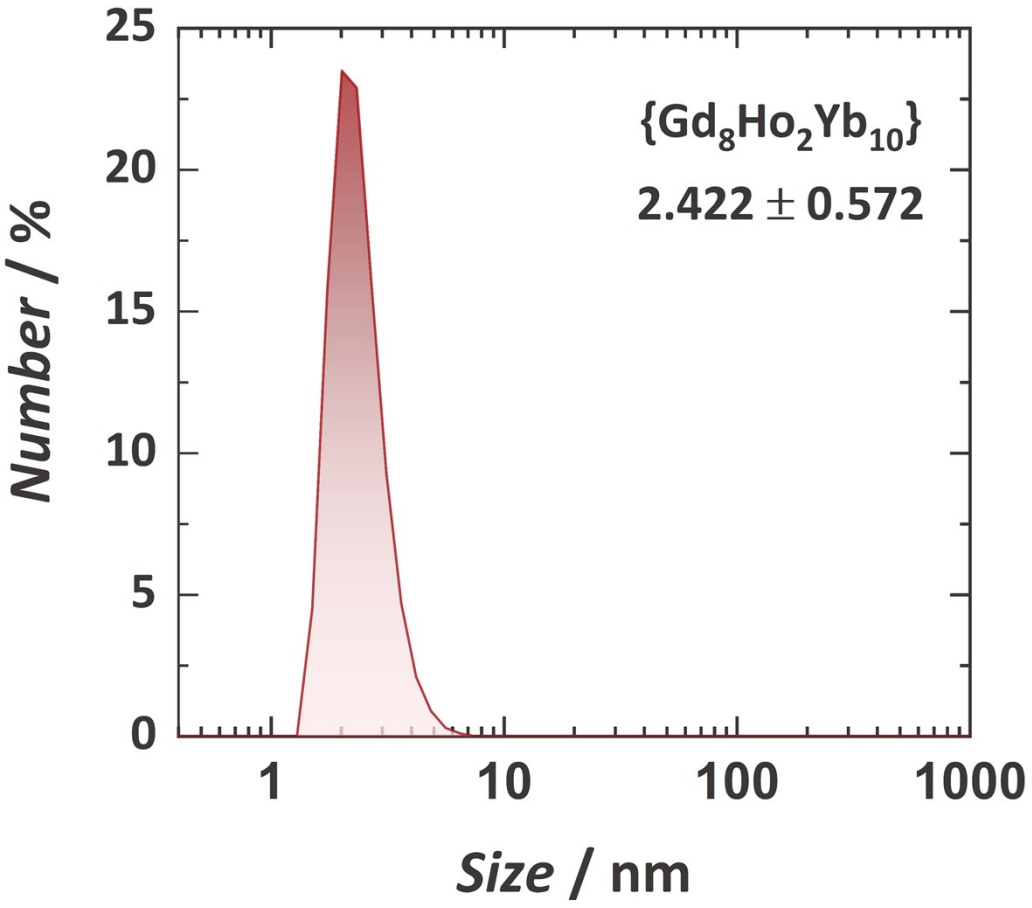

Figure S4: DLS spectra for **{$Gd_8Ho_2Yb_{10}$}** MCA obtained in deuterated methanol solution.

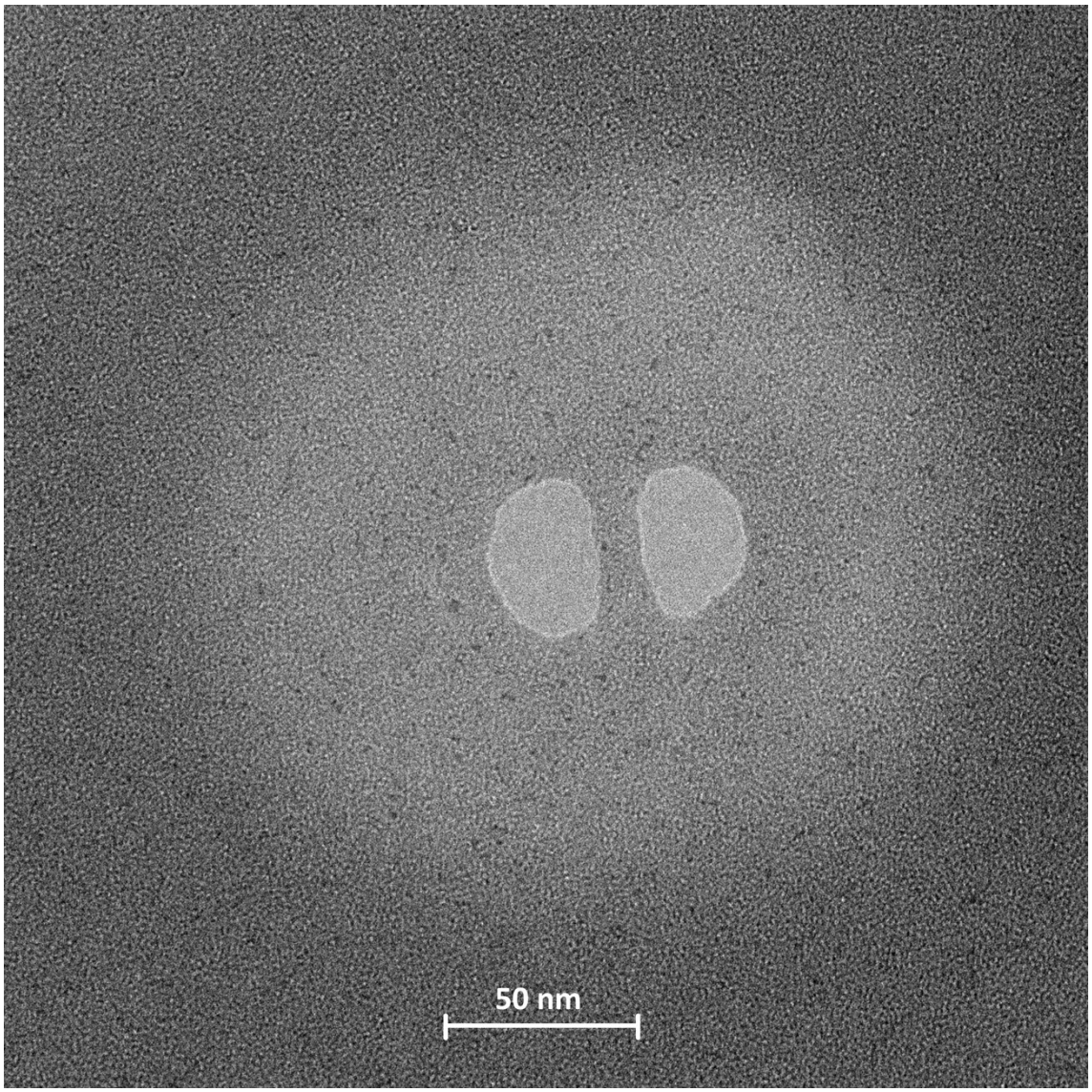

Figure S5: TEM images for **{$Gd_8Ho_2Yb_{10}$}** MCA. Due to the high ratio of organic/metal content, it is not possible to get better images with higher magnification. The low metal content (20 metal *per* molecule) significantly reduces the colour contrast. However, small spheres with diameter below 5 nm can be observed.

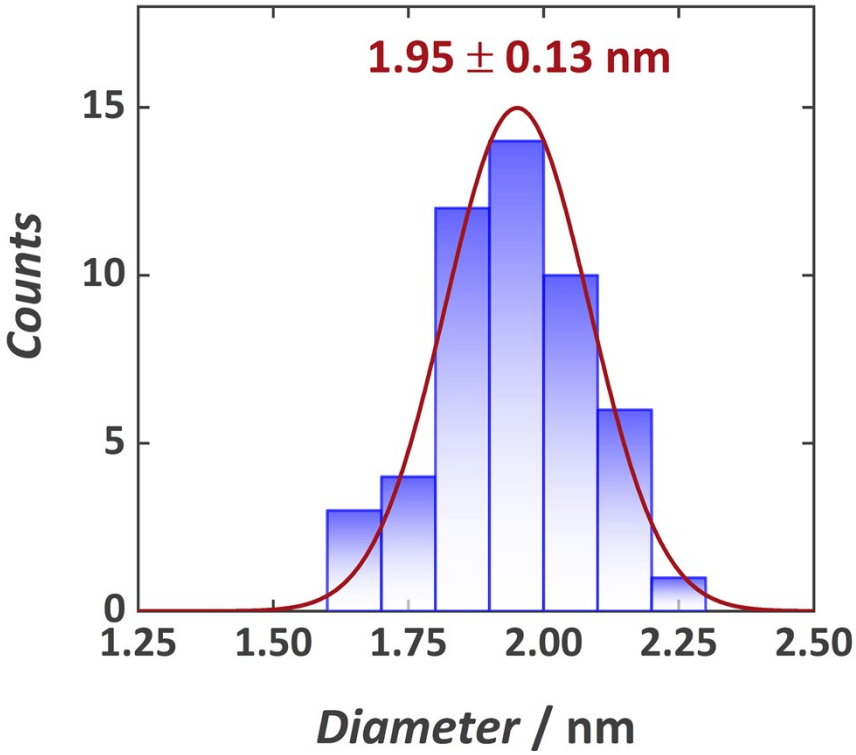

Figure S6: TEM size distribution for **{$Gd_8Ho_2Yb_{10}$}** MCA.

Figure S7: CIE diagram for **{$Gd_8Ho_2Yb_{10}$}** MCA. (P = 16 W cm^{-2}).

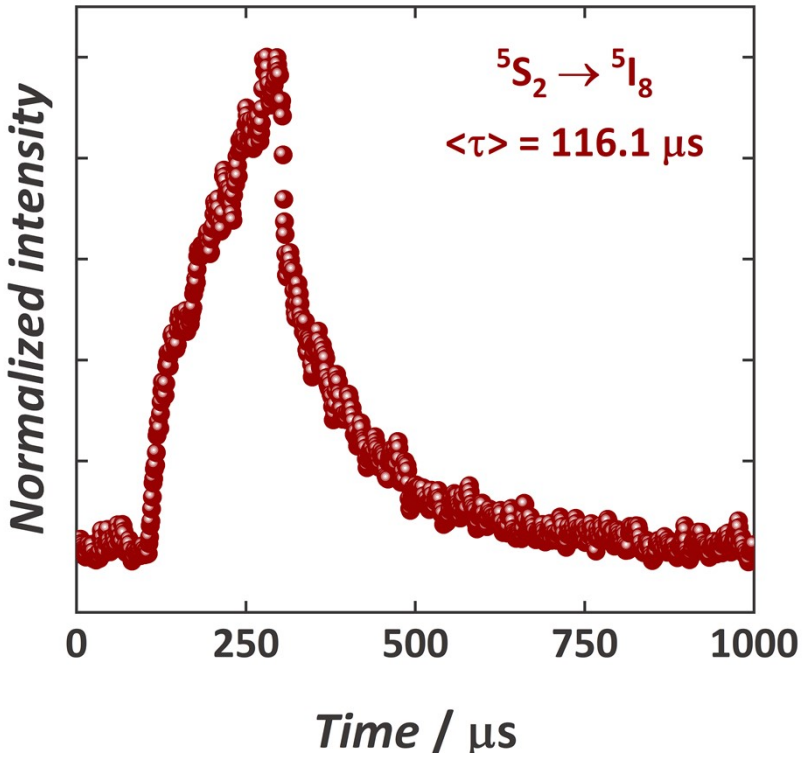

Figure S8: Upconversion decay curve for green Ho^{III} emission (550 nm) obtained at 20 °C under 980 nm laser excitation.

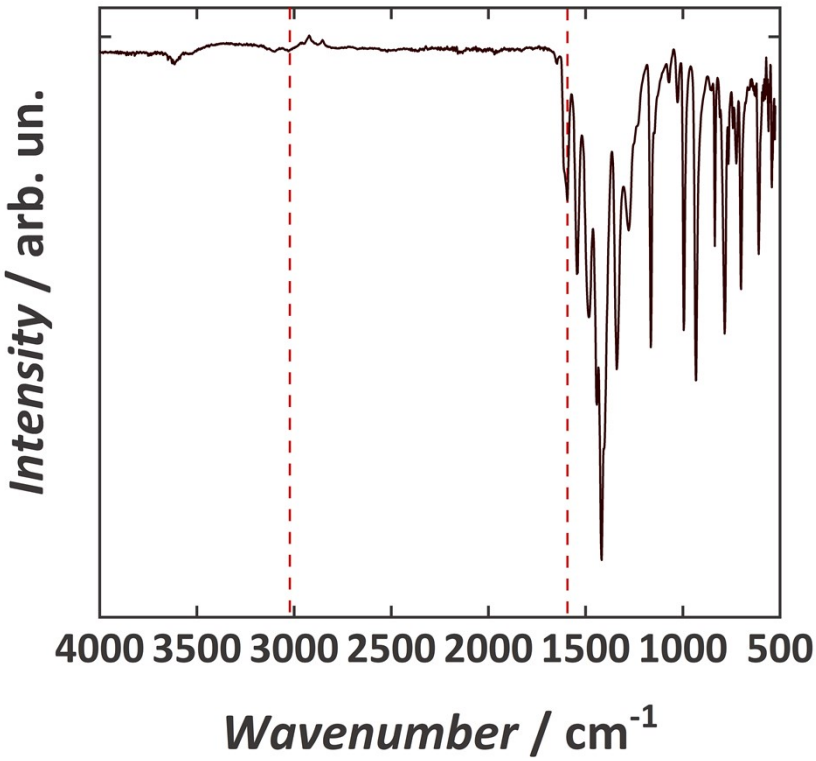

Figure S9: FTIR spectra for **{$Gd_8Ho_2Yb_{10}$}** MCA. Bands involved in couplings with important Ho^{III} electronic states are highlighted with dashed lines (see Figures S10 and S11).

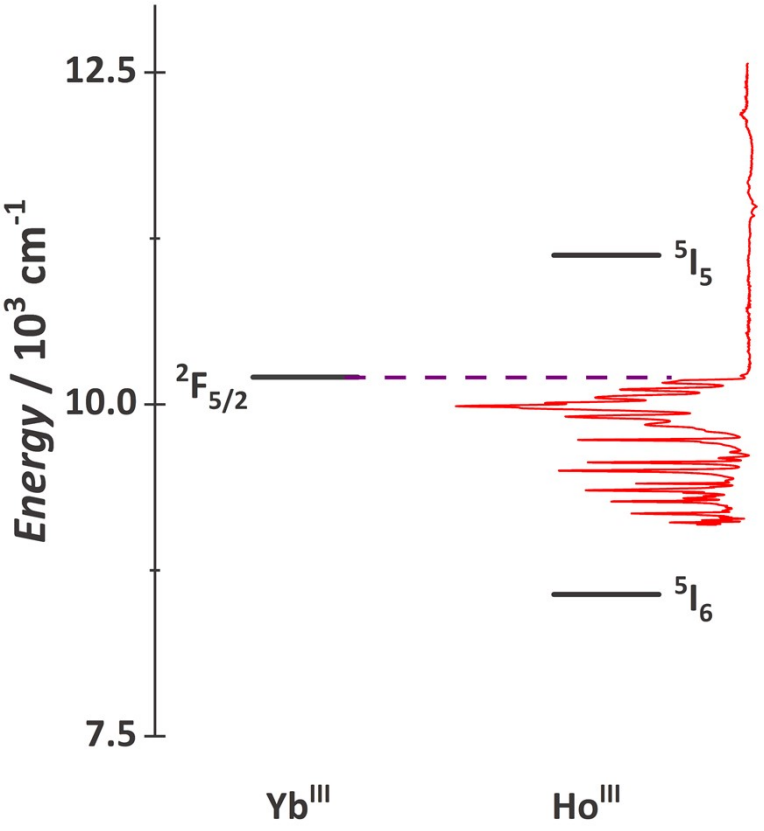

Figure S10: Vibrational coupling with Ho^{III} $^5I_6$ level.

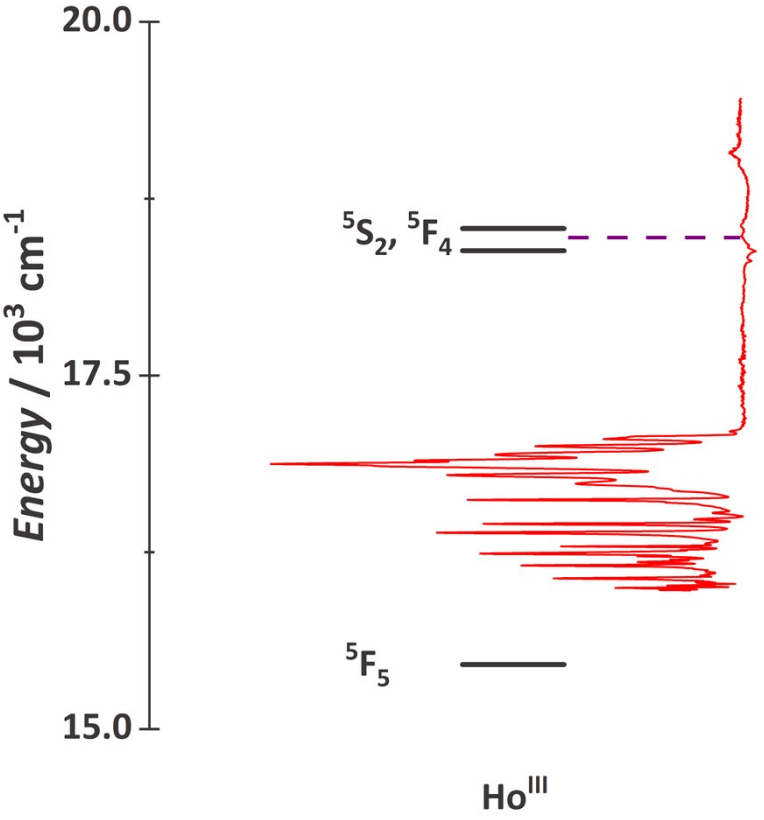

Figure S11: Vibrational coupling with Ho^{III} $^5F_5$ level.

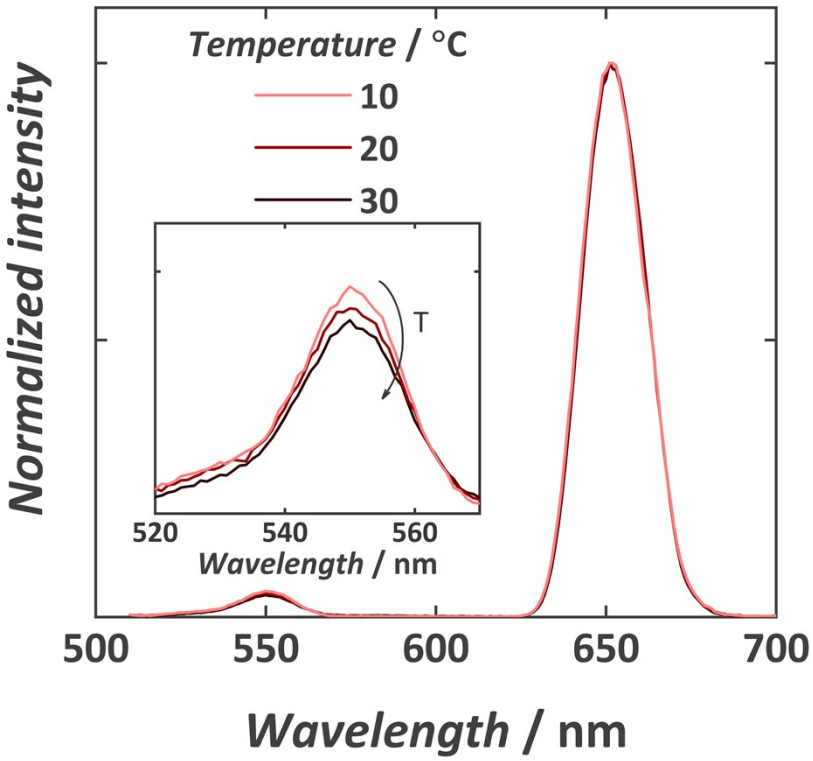

Figure S12: Temperature dependent UC spectra (P = 16 W cm^{-2}). The decrease of the green component when increasing the temperature corroborate with our proposed mechanism. With the temperature increase, the phonon-assisted mechanism induces the population of the red emitter state by deactivating the green emitter states.

References

[S1] L. Qin, G.-J. Zhou, Y.-Z. Yu, H. Nojiri, C. Schröder, R. E. P. Winpenny, Y.-Z. Zheng, *J. Am. Chem. Soc.* 2017, **139**, 16405–16411

[S2] D. A. Gálico, M. Murugesu, *ACS Appl. Mater. Interfaces* 2021, **13**, 47052–47060.